Rotational transitions induced by collisions of HD^+ ions with low-energy electrons

O. Motapon,[1,2] N. Pop,[3] F. Argoubi,[4] J. Zs Mezei,[2,5,6] M. D. Epee Epee,[1] A. Faure,[7] M. Telmini,[4]
J. Tennyson,[8] and I. F. Schneider[2,5]

[1]*LPF, UFD Mathématiques, Informatique Appliquée et Physique Fondamentale, University of Douala, P.O. Box 24157, Douala, Cameroon*
[2]*Laboratoire Ondes et Milieux Complexes, UMR 6294 CNRS and Université du Havre, 25, rue Philippe Lebon, Boite Pôstale 540, 76058 Le Havre, France*
[3]*Department of Physical Foundation of Engineering, University Politechnica of Timisoara, Bv Vasile Parvan No 2, 300223 Timisoara, Romania*
[4]*LSAMA, Department of Physics, Faculty of Science of Tunis, University of Tunis El Manar, 2092 Tunis, Tunisia*
[5]*Laboratoire Aimé Cotton CNRS-UPR-3321, Université Paris-Sud, Orsay F-91405, France*
[6]*Institute of Nuclear Research of the Hungarian Academy of Sciences, P.O. Box 51, Debrecen H-4001, Hungary*
[7]*Université UJF-Grenoble 1/CNRS-INSU, Institut de Planétologie et d'Astrophysique de Grenoble (IPAG) UMR 5274, Grenoble, France*
[8]*Department of Physics and Astronomy, University College London, London WC1E 6BT, United Kingdom*

(Received 14 March 2014; published 18 July 2014)

A series of computations based on multichannel quantum defect theory have been performed in order to produce the cross sections of rotational transitions (excitations $N_i^+ - 2 \rightarrow N_i^+$, deexcitations $N_i^+ \rightarrow N_i^+ - 2$, with $N_i^+ = 2$ to 10) and of their competitive process, the dissociative recombination, induced by collisions of HD^+ ions with electrons in the energy range 10^{-5} to 0.3 eV. Maxwell anisotropic rate coefficients, obtained from these cross sections in the conditions of the Heidelberg Test Storage Ring (TSR) experiments ($k_B T_t = 2.8$ meV and $k_B T_l = 45$ μeV), have been reported for those processes in the same electronic energy range. Maxwell isotropic rate coefficients have been presented as well for electronic temperatures up to a few hundred Kelvins. Very good overall agreement is found between our results for rotational transitions and the former theoretical computations as well as with experiment. Furthermore, due to the full rotational computations performed, the accuracy of the resulting dissociative recombination cross sections is improved considerably.

DOI: 10.1103/PhysRevA.90.012706 PACS number(s): 34.80.Gs, 34.80.Ht, 34.80.Lx, 34.50.Gb

I. INTRODUCTION

In the modeling of the kinetics of cold dilute gases, the rotational distribution of molecular species is governed by competition between formation and destruction processes, absorption, fluorescence, radiative cascades, and low-energy collisions involving neutral and ionized atomic and molecular species as well as electrons. Rate coefficients for such elementary reactions are badly needed, in particular for the chemical models of the early Universe, interstellar media, and planetary atmospheres [1–4].

Much has been done during the past years to improve the description of rotational transitions induced in molecular cations by collision with atoms or molecules. Most of the computations are based on the close-coupling technique implemented in computer codes such as MOLSCAT [5]. Meanwhile, in diffuse environments, electrons are expected to be the dominant exciting species for molecular ions as the cross sections for electron impact excitation are several orders of magnitude greater than the corresponding ones for excitation by neutral atomic or molecular species. Computations for electron-induced rotational excitation and deexcitation have been previously performed for diatomic and linear triatomic molecular ions (CH^+, HeH^+, NO^+, H_2^+, CO^+, HCO^+) [6–9], as well as polyatomic molecular ions (H_3^+, D_3^+, H_3O^+, D_3O^+, etc.) [10–13]. The theory is based on the R-matrix method [14] augmented by use of the Coulomb-Born approximation to account for long-range dipole interactions, and the adiabatic-nuclei rotation (ANR) approximation [10,15]. This method avoids consideration of an excessively large number of channels in a rotational close-coupling expansion. In the specific case of the near-threshold rotational excitation of H_3^+ by electron impact, the cross sections obtained using the ANR/R-matrix method have been shown to be in good agreement with those coming from multichannel quantum defect theory and rotation frame transformation (MQDT-RFT) [12].

The hydrogen molecular ion, which is thought to participate in the chemistry of harsh environments and considered as a key species in the formation of H_2 in the early universe [1,16], is an important subject of investigation. Its dissociative recombination (DR) together with the competing reactions—rovibrational excitation and deexcitation and dissociative excitation—play a decisive role in astrophysical ionized media (stars and interstellar molecular clouds) [1–3], fusion plasma in the divertor region [17–19], and in most of the hydrogen-containing cold plasmas of technological interest. Recent advanced studies on $H_2^+ + e^-$ [20–22] have resulted in very accurate state-to-state rate coefficients. However, the $HD^+ + e^-$ deuterated version of the $H_2^+ + e^-$ benchmark system has received more attention in storage-ring-type experiments, since its permanent dipole facilitates rapid rotational and vibrational cooling of the ion. Consequently, the dissociative recombination (DR) of HD^+,

$$HD^+ + e^- \longrightarrow H + D^*, H^* + D, \tag{1}$$

has been extensively and systematically studied both experimentally and theoretically [23–33].

More recently, the rotational cooling of HD^+ molecular ions by superelastic collisions,

$$HD^+(v_i^+ = 0, N_i^+) + e^-(\varepsilon) \longrightarrow HD^+(v_i^+ = 0, N_f^+) + e^-(\varepsilon'), \tag{2}$$

where $N_f^+ < N_i^+$, was investigated at the Test Storage Ring (TSR) of the MPIK at Heidelberg [34,35]. By merging an HD^+ beam with velocity-matched electrons, rapid cooling of the rotational excitations of the HD^+ ions by superelastic collisions (SEC) with the electrons was observed. The cooling process, which was monitored by the time evolution of the relative populations of groups of rotational levels, was well described using theoretical SEC rate coefficients obtained by combining the molecular R-matrix approach with the adiabatic nuclei rotation approximation. The present work is aimed at computing cross sections and rate coefficients for state-to-state rotational transitions (inelastic collisions and superelastic collisions) within the framework of the stepwise method based on the multichannel quantum defect theory [22,36], and then providing a comparison with the recent experiment as well as the adiabatic nuclei rotation approximation. Such data may constitute a valuable basis for a critical interpretation of the observed spectra of the species of interest [1–4]. Moreover, the results are obtained through a series of full rotational computations similar to the treatment of Ref. [22] for H_2^+, where all the relevant symmetries were appropriately considered. This provides us with improved HD^+ DR rate coefficients in comparison to our recent work [33], where the computations were restricted to the dominant $^1\Sigma_g^+$ symmetry.

This paper is organized as follows: the main steps in the computation of the cross section, based on our MQDT-type method, are reviewed in Sec. II, the computation of cross sections and rate coefficients and detailed comparison with former results are described in Sec. III, and the conclusions are provided in Sec. IV.

II. THEORETICAL METHOD

The reactive collisions between electrons and molecular cations involve *ionization* channels, describing the scattering of an electron on the molecular ion and *dissociation* channels, accounting for atom-atom scattering. The main steps of our current MQDT treatment [22] are described below.

A. Construction of the interaction matrix $\mathcal{V}$

Construction of the interaction matrix, $\mathcal{V}$, is performed in the outer shell of the region of small electron-ion and nucleus-nucleus distances, that is, in the "A-region" [37] where the Born-Oppenheimer approximation gives an appropriate description of the collision system. The good quantum numbers in this region are N, M, and Λ, associated, respectively, with the total angular momentum and its projections on the z axis of the laboratory-fixed and of the molecule-fixed frame.

Within a *quasidiabatic representation* [36,38,39], the relevant states are organized in *channels*, according to the type of fragmentation that they are meant to describe. An *ionization* channel is built starting from the ground electronic state of the ion and one of its rovibrational levels N^+v^+, and is completed by gathering all the monoelectronic states of a given orbital quantum number l. These monoelectronic states describe, *with respect to the* N^+v^+ *threshold*, either a "*free*" electron, in which case the total state corresponds to *(auto)ionization*, or to a *bound* electron, in which case the total state corresponds to a temporary *capture into a Rydberg state*. In the "A-region", these states may be modeled reasonably well with respect to the hydrogenic states in terms of the quantum defect μ_l^Λ, dependent on the internuclear distance R, but assumed to be *independent of energy*.

An ionization channel is coupled to a *dissociation* one, labeled d_j, by the electrostatic interaction $1/r_{12}$. In the molecular-orbital picture, the states corresponding to the coupled channels must differ by at least two orbitals, the dissociative states being doubly excited for the present case. We account for this coupling at the *electronic* level first, through an R-dependent *scaled* "Rydberg-valence" interaction term, $V_{d_j,l}^{(e)\Lambda}$, assumed to be *independent of the energy* of the electronic states pertaining to the ionization channel. Subsequently, the integration of this electronic interaction on the internuclear motion results in the elements of the interaction matrix $\mathcal{V}$:

$$\mathcal{V}_{d_j,lN^+v^+}^{NM\Lambda}(E,E) = \left\langle \chi_{d_j}^{N\Lambda} \middle| V_{d_j,l}^{(e)\Lambda} \middle| \chi_{N^+,v^+}^{\Lambda} \right\rangle, \tag{3}$$

where E is the total energy and $\chi_{Nd_j}^{\Lambda}$ and χ_{N^+,v^+}^{Λ} are the nuclear wave functions corresponding to a dissociative state and to an ionization channel, respectively.

This procedure applies in each Λ subspace and results in a block-diagonal global interaction matrix. The block-diagonal structure, corresponding to the Λ symmetries, propagates to the other matrices computed.

B. Construction of the reaction matrix $\mathcal{K}$

Starting from the interaction matrix $\mathcal{V}$, we build the $\mathcal{K}$-matrix, which satisfies the Lippmann-Schwinger integral equation:

$$\mathcal{K} = \mathcal{V} + \mathcal{V}\frac{1}{E - H_0}\mathcal{K}. \tag{4}$$

This equation has to be solved once $\mathcal{V}$—whose elements are given by Eq. (3)—is determined. Here H_0 is the zero-order Hamiltonian associated with the molecular system neglecting the interaction potential $\mathcal{V}$. It has been proven that, provided the electronic couplings are energy-independent, a perturbative solution of Eq. (4) is exact to the second order [40].

C. Diagonalization of the reaction matrix $\mathcal{K}$

To express the result of the short-range interaction in terms of phase shifts, we perform a unitary transformation of our initial basis into eigenstates. The columns of the corresponding transformation unitary matrix U are the eigenvectors of the K-matrix:

$$\mathcal{K}U = -\frac{1}{\pi}\tan(\eta)U, \tag{5}$$

and its eigenvalues, expressed as the nonvanishing elements of a diagonal matrix $-\frac{1}{\pi}\tan(\eta)$, provide the diagonal matrix of the phase shifts η, induced in the eigenstates by the short-range interactions.

D. Frame transformation to the external region

In the external zone—the "B-region" [37]—characterized by large electron-core distances, the Born-Oppenheimer representation is no longer valid for the whole molecule, but only

for the ionic core. Here Λ is no longer a good quantum number and a frame transformation [41–43] is performed between coupling schemes corresponding to the incident electron being decoupled from the core electrons (external region) or coupled to them (internal region). The frame transformation coefficients involve angular coupling coefficients, electronic factors, and rovibronic factors, and they are given by

$$\mathcal{C}_{lN^+v^+,\Lambda\alpha} = \left(\frac{2N^+ + 1}{2N + 1}\right)^{1/2} \langle l(\Lambda - \Lambda^+)N^+\Lambda^+ | lN^+N\Lambda\rangle \times \frac{1 + \tau^+\tau(-1)^{N-l-N^+}}{[2(2 - \delta_{\Lambda^+,0})(1 + \delta_{\Lambda^+,0}\delta_{\Lambda,0})]^{1/2}} \times \sum_v U^{\Lambda}_{lv,\alpha} \langle \chi^{\Lambda^+}_{N^+v^+} | \cos\left[\pi\mu^{\Lambda}_l(R) + \eta^{\Lambda}_{\alpha}\right] | \chi^{\Lambda}_{Nv}\rangle, \tag{6}$$

$$\mathcal{C}_{d_j,\Lambda\alpha} = U^{\Lambda}_{d_j\alpha} \cos\eta^{\Lambda}_{\alpha}, \tag{7}$$

as well as $\mathcal{S}_{lN^+v^+,\Lambda\alpha}$ and $\mathcal{S}_{d_j,\Lambda\alpha}$, which are obtained by replacing cosine with sine in Eqs. (6) and (7). In the preceding formulas, $\chi^{\Lambda^+}_{N^+v^+}$ is a vibrational wave function of the molecular ion, and χ^{Λ}_{Nv} is a vibrational wave function of the neutral system adapted to the interaction (A) region. The quantities τ^+ and τ are related to the reflection symmetry of the ion and neutral wave function, respectively, and take the values $+1$ for symmetric states and -1 for antisymmetric ones. The ratio in front of the sum on the right-hand side of Eq. (6) contains the selection rules for the rotational quantum numbers. The indices d_j ($j = 0,1,2,\ldots$) stand for the states of a given symmetry that are open to dissociation at the current energy. Here α denotes the eigenchannels built through the *diagonalization* of the reaction matrix $\mathcal{K}$, and $-\tan(\eta^{\Lambda}_{\alpha})/\pi$, $U^{\Lambda}_{lv,\alpha}$ are its eigenvalues and the components of its eigenvectors, respectively.

The projection coefficients shown in Eqs. (6) and (7) include the two types of couplings that control the process: the *electronic* coupling, expressed by the elements of the matrices $\boldsymbol{U}$ and $\boldsymbol{\eta}$, and the *nonadiabatic* coupling between the ionization channels, expressed by the matrix elements involving the quantum defect μ^{Λ}_l. This latter interaction is favored by the variation of the quantum defect with the internuclear distance R.

E. Construction of the generalized matrix X

The matrices $\boldsymbol{\mathcal{C}}$ and $\boldsymbol{\mathcal{S}}$ with the elements given by Eqs. (6) and (7) are the building blocks of the "generalized" scattering matrix $\boldsymbol{X}$:

$$\boldsymbol{X} = \frac{\boldsymbol{\mathcal{C}} + i\boldsymbol{\mathcal{S}}}{\boldsymbol{\mathcal{C}} - i\boldsymbol{\mathcal{S}}}. \tag{8}$$

It involves all the channels, open and closed. Although technically speaking only the open channels are relevant for a complete collision event, the participation of the closed channels may influence strongly the cross section, as shown below.

The $\boldsymbol{X}$ matrix relies on four block submatrices:

$$\boldsymbol{X} = \begin{pmatrix} X_{\rm oo} & X_{\rm oc} \\ X_{\rm co} & X_{\rm cc} \end{pmatrix}, \tag{9}$$

where "o" and "c" label the lines or columns corresponding to open and closed channels, respectively.

F. Elimination of closed channels

The building of the $\boldsymbol{X}$ matrix is performed independently of any account of the asymptotic behavior of the different channel wave functions. Eventually, imposing physical boundary conditions leads to the "physical" scattering matrix, restricted to the *open* channels [44]:

$$\boldsymbol{S} = \boldsymbol{X}_{\rm oo} - \boldsymbol{X}_{\rm oc}\frac{1}{\boldsymbol{X}_{\rm cc} - \exp(-i2\pi\boldsymbol{\nu})}\boldsymbol{X}_{\rm co}. \tag{10}$$

This scattering matrix is obtained from the submatrices of $\boldsymbol{X}$ appearing in Eq. (9) and from a further diagonal matrix $\boldsymbol{\nu}$ formed with the effective quantum numbers $\nu_{N^+v^+} = [2(E_{N^+v^+} - E)]^{-1/2}$ (in atomic units) associated with each vibrational threshold $E_{N^+v^+}$ of the ion situated *above* the current energy E (and consequently labeling a *closed* channel).

G. Cross-section evaluation

For a molecular ion initially on the level $N^+_i v^+_i$ and recombining with an electron of kinetic energy ε, the cross section of capture into *all* the dissociative states d_j of the same symmetry is given by

$$\sigma^{N,\rm sym}_{\rm diss\leftarrow N^+_i v^+_i} = \frac{\pi}{4\varepsilon}\frac{2N+1}{2N^+_i+1}\rho^{\rm sym}\sum_{l,\Lambda,j}\left|S^{N\Lambda}_{d_j,lN^+_iv^+_i}\right|^2. \tag{11}$$

On the other hand, the cross section for a rovibrational transition to the final level $N^+_f v^+_f$, giving collisional (de)excitation, is

$$\sigma^{N,\rm sym}_{N^+_f v^+_f\leftarrow N^+_i v^+_i} = \frac{\pi}{4\varepsilon}\frac{2N+1}{2N^+_i+1}\rho^{\rm sym}\sum_{l,l',\Lambda,j}\left|S^{N\Lambda}_{N^+_f v^+_f l',N^+_i v^+_i l}\right|^2. \tag{12}$$

Here $\rho^{\rm sym}$ is the ratio between the multiplicities of the neutral and the target ion. After performing the MQDT calculation for all the accessible total rotational quantum numbers N and for all the relevant symmetries, one has to add up the corresponding cross sections in order to obtain the global cross section for dissociative recombination or rovibrational transition, as a function of the electron collision energy ε.

III. COMPUTATION OF CROSS SECTIONS AND RATE COEFFICIENTS

A. Molecular data

Although the lowest $^1\Sigma^+_g$ doubly excited state has the most favorable crossing with the ion curve for collisions taking place at low electronic energy, a comprehensive analysis requires the consideration of the contribution of the other molecular symmetries to the cross section, especially as rotational couplings have been found to enhance superelastic and inelastic collisions in this energy range. Therefore, the molecular states that are included are $^1\Sigma^+_g$, $^1\Pi_g$, $^1\Delta_g$, $^3\Sigma^+_g$, $^3\Pi_g$, $^3\Delta_g$, $^3\Sigma^+_u$, and $^3\Pi_u$. The $^1\Sigma^+_g$ symmetry is treated simultaneously with the symmetric components with respect to the reflection symmetry of $^1\Pi_g$ and $^1\Delta_g$ to account for

rotational couplings between them. A similar treatment is used for the triplet gerade symmetries, and for $^3\Sigma_u^+$ and $^3\Pi_u$. The antisymmetric components with respect to the reflection symmetry of $^{1,3}\Pi_g$ and $^{1,3}\Delta_g$ are neglected as well as the $^1\Sigma_u^+$ and $^1\Pi_u$, because their contribution to the total cross sections is very small in comparison to the other ones.

For the $^1\Sigma_g^+$ state, we have used the adjusted quasidiabatic molecular data—electronic potential curves and couplings—previously used in Refs. [22,33]. The data for $^3\Sigma_g^+$, $^1\Delta_g$, and $^3\Delta_g$ have been obtained by combining the data of Tennyson [45] with results of new computations using the HALFIUM code developed by Telmini and Jungen [46]. In this code, the variational eigenchannel R-matrix method and the generalized multichannel quantum defect theory are combined in prolate spheroidal coordinates to determine the potential electronic energy curves of H_2. The configuration space is divided into two zones: a reaction zone and an external zone. In the inner zone, the Schrödinger equation is solved using the variational R-matrix method. The variational basis takes into account spin and σ_v symmetrizations allowing for the description of all molecular symmetries including Σ^- symmetries [47,48]. In the external zone, the hydrogen molecule is modeled as a three-body system: two positive half-charge nuclei and one electron. This approximation, called the HALFIUM model, captures the partial screening of the protons by the internal electron [49]. Matching the two expressions of the wave functions in the two zones leads to the reaction matrix, which contains the short-range interaction between the different possible channels.

Both Rydberg and doubly excited states are computed on the same footing. Thanks to the generalized MQDT formalism, all members of any Rydberg series are easily computed for an arbitrary high principal quantum number. Therefore, the quantum defects of the highest Rydberg states up to the ionization threshold are deduced in a straightforward procedure. Positions and widths of doubly excited states are obtained from resonance Breit-Wigner profiles of state density [50], and couplings are deduced from widths.

Previous results obtained for the lowest Rydberg states [46,51] agree well with the available *ab initio* data [52]. Energies and widths of doubly excited states [46,48,50,51] are also in good agreement with those of Tennyson [45]. In this work, we extended the calculations towards higher principal quantum numbers and larger internuclear distances as well. As quasidiabatic potential energy curves are needed, the closed channels are treated as open through the introduction of an artificial threshold. In this way, the data for doubly excited states including energies and couplings beyond the crossing point between these states and the molecular ion's ground-state electronic curve are obtained. Dissociation limits are deduced from the correlation diagrams [53], and extrapolation of potential energy curves is performed until the energy corresponding to the dissociation products is reached.

For each of the symmetries involved—$^{1,3}\Sigma_g^+$, $^{1,3}\Pi_g$, $^3\Sigma_u^+$, $^3\Pi_u$, and $^{1,3}\Delta_g$—only the lowest dissociative state, relevant for low-energy computation, is considered.

Two partial waves (s and d) have been taken into account for the $^1\Sigma_g^+$ state and only one partial wave for the others (d for $^1\Pi_g$, $^1\Delta_g$, $^3\Sigma_g^+$, $^3\Pi_g$, and $^3\Delta_g$, and p for $^3\Sigma_u^+$, and $^3\Pi_u$). The symmetries $^1\Delta_g$ and $^3\Delta_g$ do not have an open dissociative channel in the energy range of interest, but they contribute through the indirect mechanism via their coupling to the rotationally compatible symmetries. In practice, this is also the case for the $^3\Sigma_g^+$ symmetry, whose lowest dissociative state is open but is very weakly coupled to the ionization continuum.

B. Results and comparison with experiment

Relying on the data described above, we have performed MQDT-based [22,36] full rotational computations of the cross sections of electron-induced rotational transitions and dissociative recombination for vibrationally relaxed HD^+ molecular ions on their first 11 rotational levels ($v_i^+ = 0, N_i^+ = 0$–10), which are easily sufficient to satisfactorily model an equilibrium rotational distribution corresponding to temperatures below 1000 K. As mentioned above, rotationally compatible symmetries are treated simultaneously on the same footing.

For each initial rotational state, N_i^+, for the ion in its ground vibrational level, $v_i^+ = 0$, the cross section for the rotational transition $\sigma_{N_f^+ v_i^+ \leftarrow N_i^+ v_i^+}$ is obtained from its partial contributions $\sigma^{N,\mathrm{sym}}_{N_f^+ v_i^+ \leftarrow N_i^+ v_i^+}$ by summing them up over all the accessible values of N and all the symmetries. In a similar way, the DR cross section $\sigma_{\mathrm{diss} \leftarrow N_i^+}$ is obtained from its partial contributions $\sigma^{N,\mathrm{sym}}_{\mathrm{diss} \leftarrow N_i^+}$.

The cross sections for rotational excitations ($N_i^+ \rightarrow N_i^+ + 2$) are represented in Fig. 1, where they are compared with ones computed using the R-matrix/ANR method; see Ref. [34] for details. A zoom of the cross section for the transition $0 \rightarrow 2$ is presented in Fig. 2. The MQDT results exhibit a rich resonance structure that is due to the indirect process that is the temporary capture into the numerous Rydberg states of the neutral system (HD) involved in the process. The cross sections from the ANR approximation do not present such

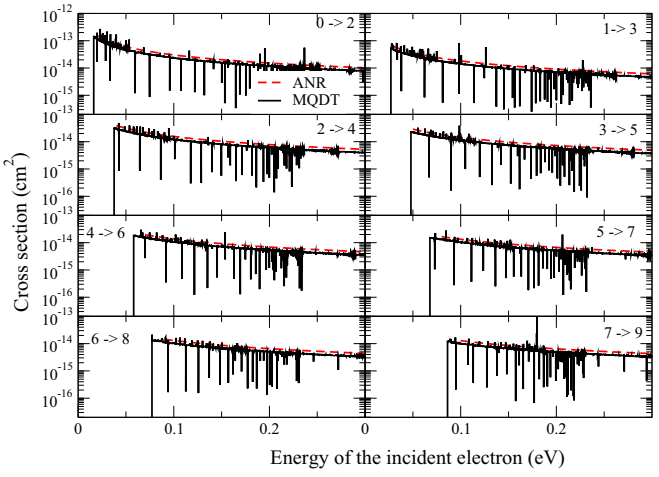

FIG. 1. (Color online) Cross sections for rotational excitations $N_i^+ - 2 \rightarrow N_i^+$, with $N_i^+ = 2$ to 9, in the ground vibrational state of $HD^+(X\,^2\Sigma_g^+)$. Black solid curves: MQDT computations; red dashed curves: ANR approximation-based computations.

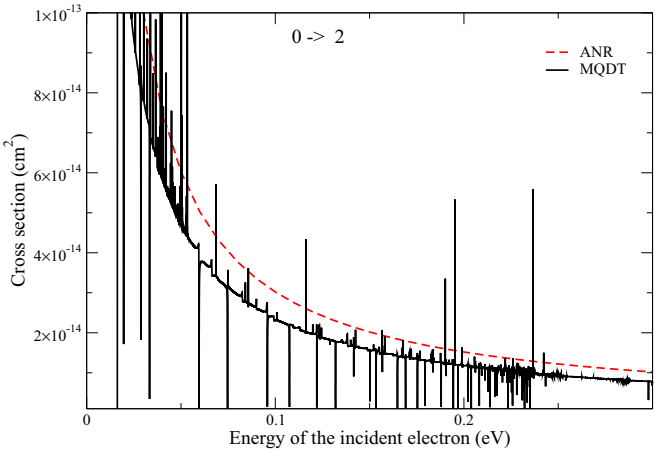

FIG. 2. (Color online) Zoom in the linear scale of the cross section for the transition $0 \rightarrow 2$, in the ground vibrational state of $HD^+(X\,^2\Sigma_g^+)$. Black solid curve: MQDT computations; red dashed curve: ANR approximation-based computations.

resonances since this approach neglects the role of the indirect process. The competition with the DR is also neglected within the ANR approach. However, in spite of the relative simplicity of this method, an overall good agreement is found between the two approaches. Nevertheless, it should be noted that the MQDT computations treat the HD molecule like H_2 from electronic point of view. Consequently, the *gerade* symmetry is completely uncoupled from the *ungerade* one and, due to selection rules inherent to the relevant partial waves [see Eq. (6)], only transitions with even ΔN^+ (0, 2, and 4) are allowed, whereas the ANR/R-matrix computations consider transitions with odd ΔN^+ (1 and 3), whose rate coefficients are not negligible but are smaller by a factor of 2 to 4.

Isotropic and anisotropic Maxwell rate coefficients were obtained for the rotational transitions by appropriate convolution of the computed cross sections. Good agreement

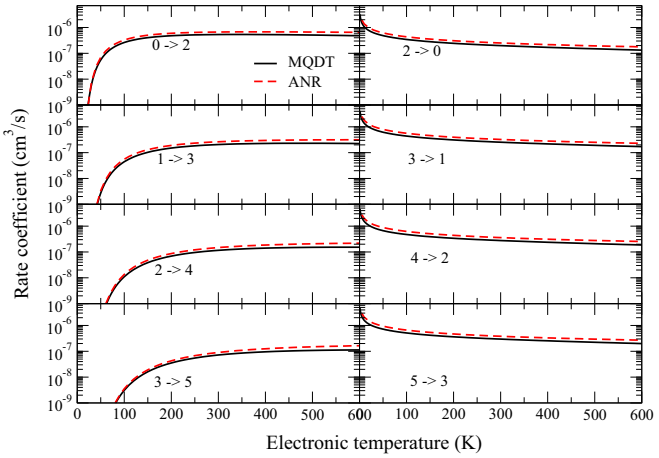

FIG. 3. (Color online) Rate coefficients of the rotational excitations $N_i^+ - 2 \rightarrow N_i^+$, with $N_i^+ = 2$ to 5, and reverse reactions, for the ground vibrational state of $HD^+(X\,^2\Sigma_g^+)$. Black solid curves: MQDT computations; red dashed curves: ANR approximation-based computations.

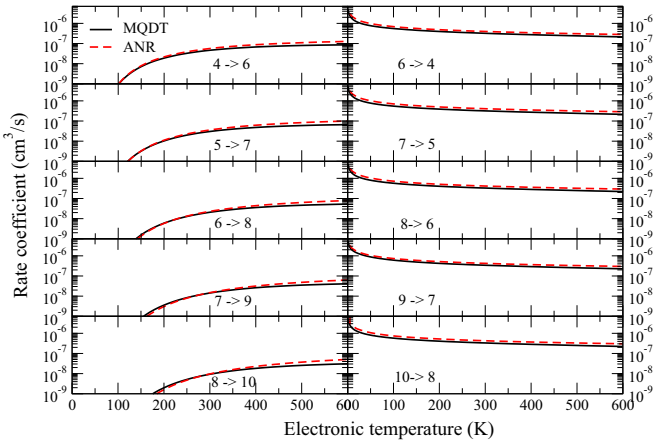

FIG. 4. (Color online) Rate coefficients of the rotational excitations $N_i^+ - 2 \rightarrow N_i^+$, with $N_i^+ = 6$ to 10, and reverse reactions for the ground vibrational state of $HD^+(X\,^2\Sigma_g^+)$. Black solid curves: MQDT computations; red dashed curves: ANR approximation-based computations.

can be observed in Figs. 3 and 4, where Maxwell isotropic rate coefficients are compared for the transitions of interest (excitation and deexcitation).

The *anisotropic* Maxwell rate coefficients at near-zero energy, obtained by convolution of the cross sections with the distribution of the relative electron-ion velocity in the latest SEC-dedicated TSR storage ring experiments [34,35] (characterized by transversal and longitudinal temperatures $k_B T_t = 2.5$ meV and $k_B T_l = 45$ μeV, respectively), are presented in Table I, and a comparison with the ANR/R-matrix calculations is performed. The values displayed are close to the average experimental rate coefficient of 1.7×10^{-6} cm^3/s found by Schwalm *et al.* [35]. The good agreement between the computed values and the measured ones confirms the dominant role of the superelastic collisions on the rotational cooling of HD^+.

Within the same MQDT computations, DR cross sections are obtained for all the rotational states of vibrationally relaxed $HD^+(X\,^2\Sigma_g^+)$ of interest in this work. Those for the first six initial rotational levels ($N_i^+ = 0$ to 5) are plotted in Figs. 5 and 6 for the energy ranges up to 24 and 300 meV, respectively. From the DR cross sections obtained, Maxwell anisotropic rate

TABLE I. Anisotropic rate coefficients for superelastic collisions of HD^+ with electrons of near-zero kinetic energy (in units of 10^{-6} cm^3/s).

Transition	MQDT (this work)	R-matrix/ANR [34,35]
$10 \rightarrow 8$	1.46	1.88
$9 \rightarrow 7$	1.57	1.85
$8 \rightarrow 6$	1.44	1.82
$7 \rightarrow 5$	1.39	1.79
$6 \rightarrow 4$	1.36	1.74
$5 \rightarrow 3$	1.28	1.67
$4 \rightarrow 2$	1.22	1.58
$3 \rightarrow 1$	1.11	1.42
$2 \rightarrow 0$	0.87	1.10

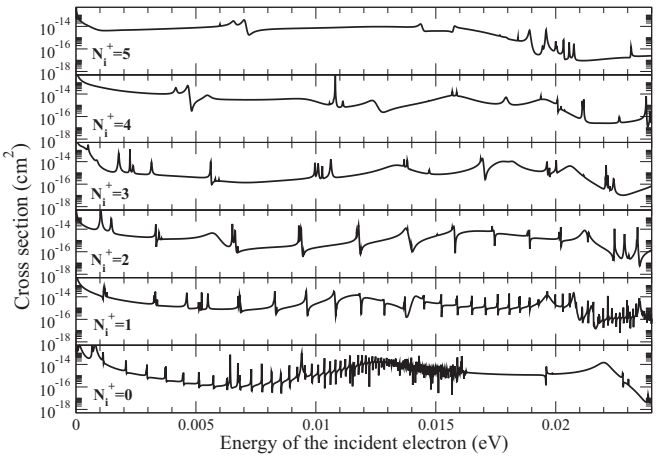

FIG. 5. Cross sections for the dissociative recombination of vibrationally relaxed $HD^+(X\,^2\Sigma_g^+)$ on initial rotational levels $N_i^+ = 0$ to 5 for electron collision energy in the range 0–24 meV.

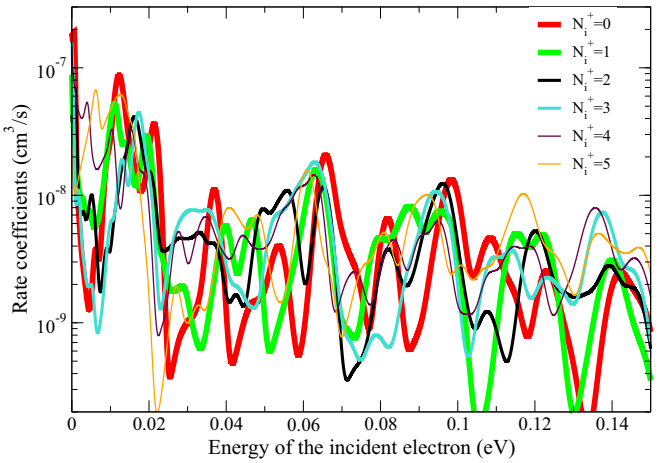

FIG. 7. (Color online) Maxwell anisotropic rate coefficients for the dissociative recombination of vibrational relaxed $HD^+(X\,^2\Sigma_g^+)$ on its initial rotational levels $N_i^+ = 0$ to 5 as in Refs. [31–33].

coefficients in the conditions of the latest DR-dedicated TSR experiments [31–33] ($k_B T_t = 2.8$ meV and $k_B T_l = 45$ μeV) have been performed in each case. The corresponding results are represented in Fig. 7 for the initial rotational levels $N_i^+ = 0$ to 5. The differences observed between the various cases enable us to appreciate the sensitivity of the cross sections to the initial rotational level. This can be accounted for by the shift in the resonance positions on the one hand, and the rotational coupling between competing molecular states from compatible symmetries on the other hand.

The quantity that needs to be computed to compare the theory with the measurements is the average Maxwell anisotropic rate coefficient, which is obtained by a weighted sum of the Maxwell anisotropic rate coefficients associated with each of the relevant initial rotational states, part of them being displayed in Fig. 7. Their weights correspond to the Boltzmann distribution associated with the assumed rotational temperature.

The results obtained have been displayed in Fig. 8, where they are compared with experiment [31,32] and our former computations [33], in which the only Rydberg-valence interaction accounted was that characterizing the $^1\Sigma_g^+$ symmetry. In Fig. 8, differences between our previous theoretical result (blue curve [33]) and the present ones (black continuous curve) at $T = 300$ K can be noted in terms of the positions and heights of some peaks. This is a consequence of the inclusion of additional symmetries, as described above, which may induce resonance shifts through their specific quantum defects, and of the mutual assistance of compatible symmetries inherent to the rotational couplings properly accounted for and which causes an attenuation in the resonant dips. The prominent peak found by the previous theoretical approach at 20 meV in agreement with the one detected by the TSR measurements shifts down to 16 meV, but its amplitude now agrees much better with the measured one. Moreover, in spite of the appearance of a prominent peak at almost zero energy and the increase in the amplitude of that already present close to 100 meV, the computed rate coefficient is closer to the measured one between 0 and 50 meV.

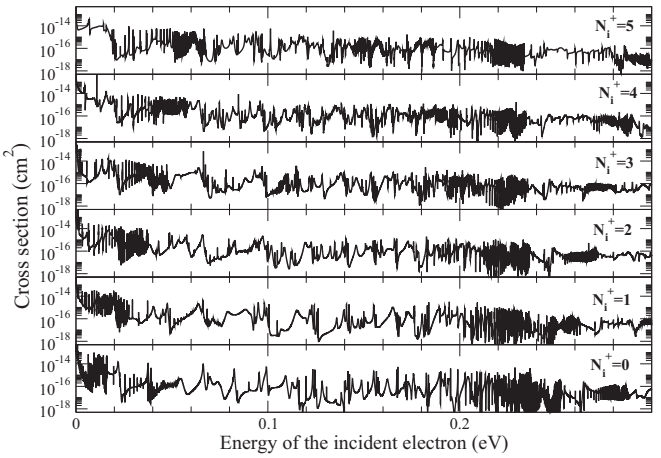

FIG. 6. Cross sections for the dissociative recombination of vibrationally relaxed $HD^+(X\,^2\Sigma_g^+)$ on initial rotational levels $N_i^+ = 0$ to 5 for electron collision energies in the range 0–300 meV.

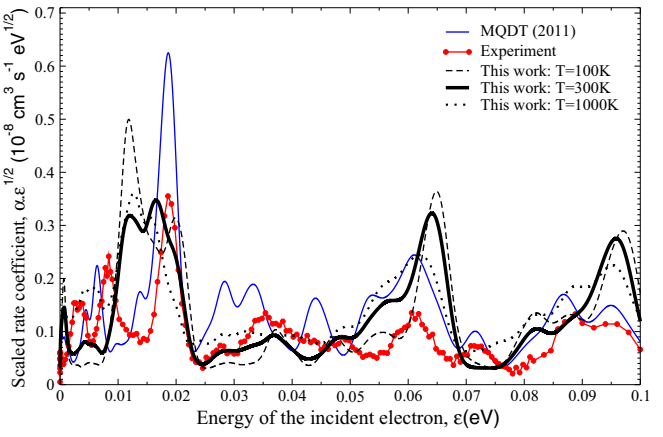

FIG. 8. (Color online) Scaled rate coefficients for the dissociative recombination of $HD^+(X\,^2\Sigma_g^+)$ at different experimental temperatures assumed for the rotational distribution of the ions in the storage ring, compared to former computations and experiment [33].

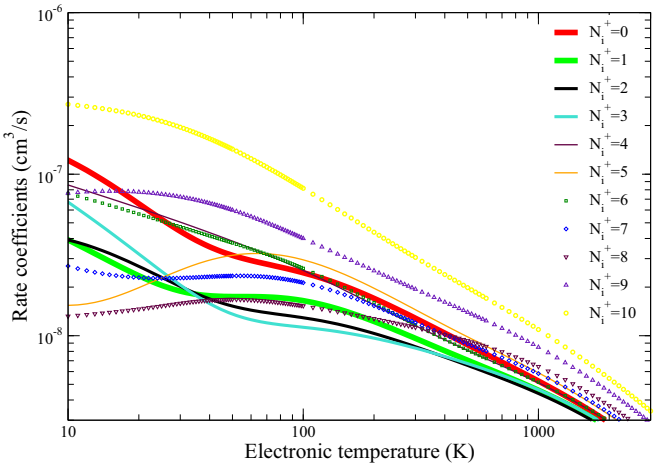

FIG. 9. (Color online) Maxwell isotropic rate coefficients for the dissociative recombination $HD^+(X\,^2\Sigma_g^+)$ with $v_i^+ = 0$ as a function of initial rotational level, $N_i^+ = 0$ to 10 .

Since there is still some uncertainty in the rotational temperature of the cation in the storage ring, we compute and display in Fig. 8 the rate coefficient for 100 and 1000 K, besides that for 300 K. Indeed, one may notice that for $T = 1000$ K, the agreement with experiment is better in terms of cross-section amplitudes than that for $T = 300$ K below 10 meV and between 50 and 70 meV. For $T = 100$ K, the agreement is better in the energy range 25–60 meV. This may mean that the occupation probability of the rotational levels is not a simple Maxwell-Boltzmann distribution, i.e., temperature-dependent, but it includes some dependence on the energy of the incident electron, perhaps via inelastic and mainly superelastic collisions.

For further use in astrochemistry and cold plasmas modeling, we have performed *isotropic* Maxwell convolution from all the cross sections computed. The corresponding isotropic rate coefficients are plotted in Fig. 9 for all the initial rotational levels. These results show that above the initial rotational state $N_i^+ = 6$, rotational excitation of the target favors dissociative recombination in the sense that the DR rate coefficients increase with increasing N_i^+. In contrast, below $N_i^+ = 6$, rotational excitation slows down DR.

IV. CONCLUSION

A series of computations have been carried out for the collisions between HD^+ molecular ions and electrons with kinetic energy below 300 meV. Whereas in our previous calculations on this species [33] the only Rydberg-valence interactions considered were those within the dominant symmetry $^1\Sigma_g^+$, in the present ones this symmetry contributes simultaneously with the "+" components of the $^1\Pi_g$ and $^1\Delta_g$ symmetries, the corresponding states being rotationally coupled. Moreover, we have involved in the same way in the present approach the triplet gerade, and the singlet and triplet ungerade symmetries. The account of these numerous states and interactions makes the current treatment more accurate than the previous ones. A further step in the same direction will be the use of more accurate molecular data. This will be achieved by using the latest and ongoing progress in the *R*-matrix and MQDT techniques [47,54,55] in producing potential energy curves and electronic couplings, which can be used to produce realistic models (positions, amplitudes, and widths) for the Rydberg resonances dominating the shape of the cross sections. An alternative route to improved accuracy is the use of the global version of the MQDT [56], which has proved its efficiency in the spectroscopy of the neutral H_2 and its isotopes [57].

Cross sections and Maxwell anisotropic and isotropic rate coefficients have been obtained for state-to-state rotational transitions induced in HD^+ molecular ions by electronic collisions. At very low collision energy, the Maxwell anisotropic rate coefficients computed with both MQDT and ANR/*R*-matrix methods are in good agreement. They are comparable to within 30% with those resulting from a fit of the experimental cooling curves, derived from the the measurements performed at the Heidelberg Test Storage Ring [35]. These latter results account for the strong contribution of the rotational deexcitation to the rotational cooling of HD^+ molecular ions, as reported by Shafir *et al.* [34] and Schwalm *et al.* [35].

Furthermore, cross sections and Maxwell anisotropic and isotropic rate coefficients have been derived for the dissociative recombination of HD^+ molecular ions. In spite of the displacement of few prominent resonances with respect to the previous predicted positions and/or with respect to the positions found by the measurements, the agreement between theory and experiment has been improved at low energy. The numerical data for all the initial $N_i^+ = 0$ to 10, ready to be used in the kinetics modeling in astrochemistry and cold plasma physics, are available upon request. Similar computations are ongoing for the H_2^+ and D_2^+ molecular ions, and the corresponding results will be reported in a future article.

ACKNOWLEDGMENTS

The authors thank A. Wolf, D. Schwalm, D. Dowek, Ch. Jungen, H. Takagi, and S. L. Guberman for numerous discussions, and S. Ilie for technical assistance. Some of the molecular data used in the computations have been produced with the use of the LAC-MQDT package of codes of Ch. Jungen. O.M. is grateful to the International Atomic Energy Agency (IAEA, Vienna) for financial support through Contract No 16712 with the University of Douala (CAMEROON). The authors acknowledge scientific and financial support from the IAEA, via the Coordinated Research Projects "Atomic and Molecular Data for State-Resolved Modelling of Hydrogen and Helium and their Isotopes in Fusion Plasmas," and "Light Element Atom, Molecule and Radical Behaviour in the Divertor and Edge Plasma Regions"), as well as from the European Spatial Agency (ESA) via Contract No. ESTEC 21790/08/NL/HE. We are grateful for the financial support from the French Research Federation for Fusion Studies (CEA, EFDA, EURATOM), from Agence Nationale de la Recherche via the projects "SUMOSTAI" (ANR-09-BLAN-020901) and "HYDRIDES" (ANR-12-BS05-0011-01), from the IFRAF-Triangle de la Physique via the project "SpecoRyd," and from

the CNRS via the programme "Physique et Chimie du Milieu Interstellaire" and the CNRS PEPS projects "Physique théorique et ses interfaces" TheMS and TPCECAM. We gratefully acknowledge the generous financial support from La Région Haute-Normandie via the CPER "THETE" project, and the GRR Electronique, Energie et Matériaux. Part of this work has been performed in the frame of the "Fédération de Recherche Energie, Propulsion, Environnement," and of the LabEx EMC^3, via the project PicoLIBS (ANR-10-LABX-09-01).

[1] C. M. Coppola, S. Longo, M. Capitelli, F. Palla, and D. Galli, Astrophys. J. Suppl. Ser. **193**, 7 (2011).

[2] F. Le Petit, E. Roueff, and J. Le Bourlot, Astron. Astrophys. **390**, 369 (2002); E. Roueff and F. Le Petit, in *Astrochemistry: Recent Successes and Current Challenges*, Proceedings of the IAU Symposium No. 231, edited by D. C. Lis, G. A. Blake, and E. Herbst (Cambridge University Press, Cambridge, 2006), p. 197; M. Agúndez, J. R. Goicoechea, J. Cernicharo, A. Faure, and E. Roueff, Astrophys. J. **713**, 662 (2010).

[3] J. H. Black and A. Dalgarno, Astrophys. J. **203**, 132 (1976); E. F. Van Dishoeck and J. H. Black, Astrophys. J. Suppl. Ser. **62**, 109 (1986); J. H. Black and E. F. Van Dishoeck, Astrophys. J. **322**, 412 (1987).

[4] C. D. Gay, N. P. Abel, R. L. Porter, P. C. Stancil, G. J. Ferland, G. Shaw, P. A. M. Van Hoof, and R. J. R. Williams, Astrophys. J. **746**, 78 (2012).

[5] J. M. Hutson and S. Green, MOLSCAT computer code, version 14 (UK: Collaborative Computation Project No. 6 of the Science and Engineering Council, 1994).

[6] I. Rabadán, B. K. Sarpal, and J. Tennyson, Mon. Not. R. Astron. Soc. **299**, 171 (1998).

[7] A. J. Lim, I. Rabádan, and J. Tennyson, Mon. Not. R. Astron. Soc. **306**, 473 (1999).

[8] A. Faure and J. Tennyson, Mon. Not. R. Astron. Soc. **325**, 443 (2001).

[9] I. Jimenez-Serra, J. Martin-Pintado, S. Viti, S. Martin, A. Rodriguez-Franco, A. Faure, and J. Tennyson, Astrophys. J. **650**, L135 (2006).

[10] A. Faure and J. Tennyson, J. Phys. B **35**, 3945 (2002).

[11] A. Faure and J. Tennyson, Mon. Not. R. Astron. Soc. **340**, 468 (2003).

[12] A. Faure, V. Kokoouline, C. H. Greene, and J. Tennyson, J. Phys. B **39**, 4261 (2006).

[13] V. Kokoouline, A. Faure, J. Tennyson, and C. H. Greene, Mon. Not. R. Astron. Soc. **405**, 1195 (2010).

[14] J. Tennyson, Phys. Rep. **491**, 29 (2010).

[15] I. Rabadán and J. Tennyson, Comput. Phys. Commun. **114**, 129 (1998).

[16] J. M. C. Rawlings, J. E. Drew, and M. J. Barlow, Mon. Not. R. Astron. Soc. **265**, 968 (1993).

[17] R. T. Janev, *Atomic and Molecular Processes in Fusion Edge Plasmas* (Plenum, New York, 1995).

[18] D. Reiter, in *Nuclear Fusion Research: Understanding Plasma Surface Interaction*, edited by R. E. H. Clarke and D. Reiter (Springer, Heidelberg, 2005), p. 29.

[19] U. Fantz, D. Reiter, B. Heger, and D. Coster, J. Nucl. Mat. **290–293**, 367 (2001); U. Fantz and P. T. Greenland, Contrib. Plasma Phys. **42**, 694 (2002); U. Fantz and D. Wunderlich, in *Atomic and Plasma-Material Interaction Data for Fusion* (International Atomic Energy Agency, Vienna, 2008), Vol. 14, p. 56; U. Fantz and D. Wunderlich, in *Atomic and Plasma-Material Interaction Data for Fusion* (International Atomic Energy Agency, Vienna, 2011), Vol. 16, p. 76.

[20] V. Zhaunerchyk, A. Al-Khalili, R. D. Thomas, W. D. Geppert, V. Bednarska, A. Petrignani, A. Ehlerding, M. Hamberg, M. Larsson, S. Rosen, and W. J. van der Zande, Phys. Rev. Lett. **99**, 013201 (2007).

[21] N. de Ruette, Ph.D. thesis, Université Catholique de Louvain la Neuve, 2007, http://hdl.handle.net/2078.1/6251.

[22] O. Motapon, F. O. Waffeu Tamo, X. Urbain, and I. F. Schneider, Phys. Rev. A **77**, 052711 (2008).

[23] P. Forck, M. Grieser, D. Habs, A. Lampert, R. Repnow, D. Schwalm, A. Wolf, and D. Zajfman, Phys. Rev. Lett **70**, 426 (1993).

[24] T. Tanabe, I. Katayama, H. Kamegaya, K. Chida, Y. Arakaki, T. Watanabe, M. Yoshizawa, M. Saito, Y. Haruyama, K. Hosono, K. Hatanaka, T. Honma, K. Noda, S. Ohtani, and H. Takagi, Phys. Rev. Lett. **75**, 1066 (1995).

[25] C. Stromholm, I. F. Schneider, G. Sundstrom, L. Carata, H. Danared, S. Datz, O. Dulieu, A. Kallberg, M. afUgglas, X. Urbain, V. Zengin, A. Suzor-Weiner, and M. Larsson, Phys. Rev. A **52**, R4320 (1995).

[26] J. R. Mowat, H. Danared, G. Sundstrom, M. Carlson, L. H. Andersen, L. Vejby-Christensen, M. afUgglas, and M. Larsson, Phys. Rev. Lett. **74**, 50 (1995).

[27] I. F. Schneider, C. Strömholm, L. Carata, X. Urbain, M. Larsson, and A. Suzor-Weiner, J. Phys. B **30**, 2687 (1997).

[28] Z. Amitay, A. Baer, M. Dahan, L. Knoll, M. Lange, J. Levin, I. F. Schneider, D. Schwalm, A. Suzor-Weiner, Z. Vager, R. Wester, A. Wolf, and D. Zajfman, Science **281**, 75 (1998).

[29] Z. Amitay, A. Baer, M. Dahan, J. Levin, Z. Vager, D. Zajfman, L. Knoll, M. Lange, D. Schwalm, R. Wester, A. Wolf, I. F. Schneider, and A. Suzor-Weiner, Phys. Rev. A **60**, 3769 (1999).

[30] H. Takagi, Phys. Scr. **T96**, 52 (2002).

[31] A. Al-Khalili, S. Rosen, H. Danared, A. M. Derkatch, A. Kallberg, M. Larsson, A. LePadellec, A. Neau, J. Semaniak, R. Thomas, M. afUgglas, L. Vikor, W. Zong, W. J. van der Zande, X. Urbain, M. J. Jensen, R. C. Bilodeau, O. Heber, H. B. Pedersen, C. P. Safvan, L. H. Anderson, M. Lange, J. Levin, G. Gwinner, L. Knoll, M. Scheffel, D. Schwalm, R. Wester, D. Zajfman, and A. Wolf, Phys. Rev. A **68**, 042702 (2003).

[32] H. Buhr, Ph.D. thesis, University of Heidelberg, 2006.

[33] F. O. Waffeu Tamo, H. Buhr, O. Motapon, S. Altevogt, V. M. Andrianarijaona, M. Grieser, L. Lammich, M. Lestinsky, M. Motsch, I. Nevo, S. Novotny, D. A. Orlov, H. B. Pedersen, D. Schwalm, F. Sprenger, X. Urbain, U. Weigel, A. Wolf, and I. F. Schneider, Phys. Rev. A **84**, 022710 (2011).

[34] D. Shafir *et al.*, Phys. Rev. Lett. **102**, 223202 (2009).

[35] D. Schwalm *et al.*, J. Phys.: Conf. Ser. **300**, 012006 (2011).

[36] A. Giusti-Suzor, J. Phys. B **13**, 3867 (1980).

[37] Ch. Jungen and O. Atabek, J. Chem. Phys. **66**, 5584 (1977).

[38] N. Bardsley, J. Phys. B **1**, 349 (1968); **1**, 365 (1968).

[39] V. Sidis and H. Lefebvre-Brion, J. Phys. B **4**, 1040 (1971).

[40] V. Ngassam, A. Florescu, L. Pichl, I. F. Schneider, O. Motapon, and A. Suzor-Weiner, Eur. Phys. J. D **26**, 165 (2003).

[41] B. Vâlcu, I. F. Schneider, M. Raoult, C. Strömholm, M. Larsson, and A. Suzor-Weiner, Eur. Phys. J. D **1**, 71 (1998).
[42] U. Fano, Phys. Rev. A **2**, 353 (1970).
[43] E. S. Chang and U. Fano, Phys. Rev. A **6**, 173 (1972).
[44] M. J. Seaton, Rep. Prog. Phys. **46**, 167 (1983).
[45] J. Tennyson, At. Data. Nucl. Data Tables **64**, 253 (1996).
[46] M. Telmini and Ch. Jungen, Phys. Rev. A **68**, 062704 (2003).
[47] F. Argoubi, S. Bezzaouia, H. Oueslati, M. Telmini, and Ch. Jungen, Phys. Rev. A **83**, 052504 (2011).
[48] S. Bezzaouia, F. Argoubi, M. Telmini, and Ch. Jungen, J. Phys.: Conf. Ser. **300**, 012013 (2011).
[49] S. Bezzaouia and M. Telmini, in *Fundamental and Applied Spectroscopy: Second International Spectroscopy Conference*, edited by M. Telmini, N. T. Mliki, and E. Sediki, AIP Conf. Proc. No. 935 (AIP, New York, 2007), p. 183.
[50] M. Telmini, S. Bezzaouia, and Ch. Jungen, Int. J. Quantum Chem. **104**, 530 (2005).
[51] S. Bezzaouia, M. Telmini, and Ch. Jungen, Phys. Rev. A **70**, 012713 (2004).
[52] W. Kolos and L. Wolniewicz, J. Chem. Phys. **50**, 3228 (1969); L. Wolniewicz and K. Dressler, *ibid.* **100**, 444 (1994); T. Orlikowski, G. Staszewska, and L. Wolniewicz, Mol. Phys. **96**, 1445 (1999).
[53] T. E. Sharp, At. Data. Nucl. Data Tables **2**, 119 (1970); I. Sanchez and F. Martín, J. Chem. Phys. **106**, 7720 (1997).
[54] D. A. Little and J. Tennyson, J. Phys. B **47**, 105204 (2014).
[55] H. Oueslati, F. Argoubi, S. Bezzaouia, M. Telmini, and Ch. Jungen, Phys. Rev. A **89**, 032501 (2014).
[56] Ch. Jungen, in *Elements of Quantum Defect Theory*, Handbook of High-resolution Spectroscopy, edited by M. Quack and F. Merkt (Wiley, New York, 2011), p. 471.
[57] J. Zs. Mezei, I. F. Schneider, E. Roueff, and Ch. Jungen, Phys. Rev. A **85**, 043411 (2012).